Flexible Hybrid Electronic Circuits and Systems

David E. Schwartz, Jonathan Rivnay, Gregory L. Whiting, Ping Mei, Yong Zhang, Brent Krusor, Sivkheng Kor, George Daniel, Steve E. Ready, Janos Veres, and Robert A. Street

***Abstract*— Printed organic electronics are being explored for a wide range of possible applications, with much of the current focus on smart labels, wearables, health monitoring, sensors and displays. These applications typically integrate various types of sensors and often include silicon integrated circuits (IC) for computation and wireless communications. Organic thin film transistors (TFT), particularly when printed, have performance and yield limitations that must be accommodated by the circuit design. The circuit design also needs to select sensor technology, ICs and other circuit elements to integrate with the TFTs and match the functional and performance requirements of the application. This paper describes organic TFT properties and strategies for circuit and sensor design, with examples from various sensor systems.**

***Index Terms*— Hybrid circuits, organic transistors, printed electronics.**

I. Introduction

ORGANIC electronics, as an emerging technology, has potential applications in flexible displays [1], smart labels [2], wearable electronics [3], soft robotics [4], and prosthetics [5]. While conventional electronics are fabricated on rigid, inorganic substrates, organics are compatible with plastic film substrates that are flexible, soft, and stretchable, thus enabling conformal integration with curvilinear objects. In addition, manufacturing by printing is scalable to large areas and is amenable to low-cost sheet-fed and roll-to-roll processes.

Printed organic electronics (POE) include display and sensory components to interface with users and environments. On the systems level, however, POE also requires electronic circuits for power, memory, signal conditioning, and communications. All of the aforementioned electronic components can be integrated on plastic substrates by either assembly or printing. In the assembly approach, conventionally fabricated integrated circuit (IC) chips or bare dies are transferred to plastic substrates via robotic pick and place. Although it introduces local mechanical rigidity to POE systems, this hybrid approach takes advantage of high-performance electronic materials and high-resolution patterning techniques available in microfabrication, making it suitable for applications that require high-performance electronics.

In contrast, the printing approach fabricates circuit elements digitally by dispensing liquid inks of desired conducting, semiconducting, dielectric, and optical properties onto plastic substrates. Printing tends to result in moderate-performance circuits owing to the available semiconductor inks and low patterning resolution. Despite these shortcomings, the all-printed approach takes full advantage of POE and hence can enable commercial applications in high throughput, disposable, or highly customizable electronics.

Progress in ink development and printing techniques have significantly improved the performance of printable electronic materials. However, there remain some device performance issues that are intrinsic to POE. For example, while thin film transistors (TFTs) have been printed with organic semiconductors that are comparable to amorphous Si in mobility, arrays of TFTs typically have large variations in mobility and threshold voltages. Fortunately, those challenges can be mitigated from a circuit design perspective. This paper presents the printing and design considerations of circuit components, followed by the descriptions of a few exemplary POE systems.

II. Organic and printed TFTs

Organic semiconductors are a natural transistor material for printed and flexible electronics. They are soluble, have low processing temperatures compatible with plastic substrates, and their low elastic modulus is consistent with mechanical flexibility. Deposition processes by printing or various solution coating techniques are relatively simple and therefore potentially inexpensive. Their mobility has been steadily increasing over the past 10–20 years, and now reaches $\sim$5 cm^2/Vs, with some reports of higher mobility. There are both p-channel and n-channel TFTs enabling complementary circuit design, although p-channel TFTs have been studied for longer and more semiconductor materials have been developed. The small molecule solution form of pentacene [6] for n-channel devices, and new polymers of the polythiophene family [7] for p-channel TFTs are common examples. There are other printable materials that form high mobility TFTs, such as metal oxides [8] and carbon nanotubes [9] that could replace the organics. Both top and bottom gate organic TFTs are possible but the trend is towards top gate, in part because the gate dielectric offers encapsulation of the organic semiconductor which is often degraded by exposure to the ambient. In keeping with solution processing, there are many possible organic gate dielectrics and printable nanoparticle metals for interconnects as well as source, drain and gate contacts. TFTs with both top and bottom gates can enhance circuit performance [10].

Organics have a low dielectric constant and printing techniques such as ink-jet are limited to larger feature size than for typical large area conventional lithography. The effect of these constraints are TFTs with long channel length, low transconductance, high parasitic capacitance and high operating voltages, which often significantly limit the

Manuscript received April 15, 2016; revised July 21, 2016; accepted September 11, 2016. Date of publication October 18, 2016; date of current version March 15, 2017. This work was supported in part by Xerox, in part by the Defense Advanced Research Projects Agency, in part by Nano-Bio Manufacturing Consortium, in part by FlexTech, in part by Advanced Research Projects Agency-Energy, and in part by Thin Film Electronics. This paper was recommended by Guest Editor J. Chang.

The authors are with Palo Alto Research Center – a Xerox company, Palo Alto, CA 94304 USA.

Color versions of one or more of the figures in this paper are available online at http://ieeexplore.ieee.org.

Digital Object Identifier 10.1109/JETCAS.2016.2612623

performance of circuits. A number of ways to improve the TFT performance have been developed. High dielectric constant or very thin dielectrics increase the gate capacitance and reduce operating voltages. In particular PVDF copolymers can be used as a solution processable dielectric with a dielectric constant up to 40 in some cases. Thin gate dielectrics that reduce the TFT operating voltage to $\sim$ 3V have also been demonstrated, but may be susceptible to pin-hole defects. Solid electrolyte gate dielectrics have a high effective dielectric constant, also leading to reduced operating voltage [11]. Parasitic capacitance arises primarily from the overlap of gate and source-drain electrodes, and is particularly large in many printed devices because of the low printing resolution. Lithographically defined TFTs with much finer lines give significantly improved characteristics. Printing techniques capable of fine features for at least the source and drain contacts improves the circuit performance and a robust self-aligned TFT process would be a significant improvement.

Contact resistance has been another issue for organic TFTs. It is often observed that the apparent mobility decreases with the channel length, so that the expected circuit performance gain with reduced channel length is not achieved. The problem arises because the organic semiconductor generally cannot be doped effectively and so a low contact resistance relies on matching the metal work function to the organic semiconductor. Shorter channel length requires better matching because of the increased current. Fortunately coatings such as F4TCNQ and PEIE can be used that modify the metal work function and the use of these has reduced the issue [12].

Organic TFTs exhibit degradation both by exposure to the atmosphere and in operation with prolonged gate bias, again with significant implications for circuit performance and stability. Reversible bias stress is due to charge trapping either in the channel or in the gate dielectric [13], and its magnitude is comparable to or better than that of amorphous silicon TFTs. Irreversible threshold voltage shifts due to chemical degradation [14] are a further source of time dependent variability and require good encapsulation of devices.

Fig. 1 shows some examples of ink-jet printed organic TFT characteristics and illustrates the substantial device-to-device variation that can occur in nominally identical devices. The curves in Fig. 1 a are of nominally identical devices, yet currents vary by up to 50% from the mean. Fig. 1(b) and (c) shows histograms of measured on current and on/off ratio, respectively. Variations can arise from inconsistently printed electrode spacing, as well as morphology and thickness variations in the semiconductor. Improvements in each of these properties can be expected with better control of material and printing, but such a variation is a common observation [15], [16]. Section III discusses how device variations are taken into account in circuit modeling. Both TFT variability and yield issues such as misprints, contamination, and other factors necessitates a circuit design strategy that minimizes the number of devices.

Additive printing of TFTs combines patterning and deposition into a single step and requires printers capable of accurately registering multiple patterned layers. Jet-printing

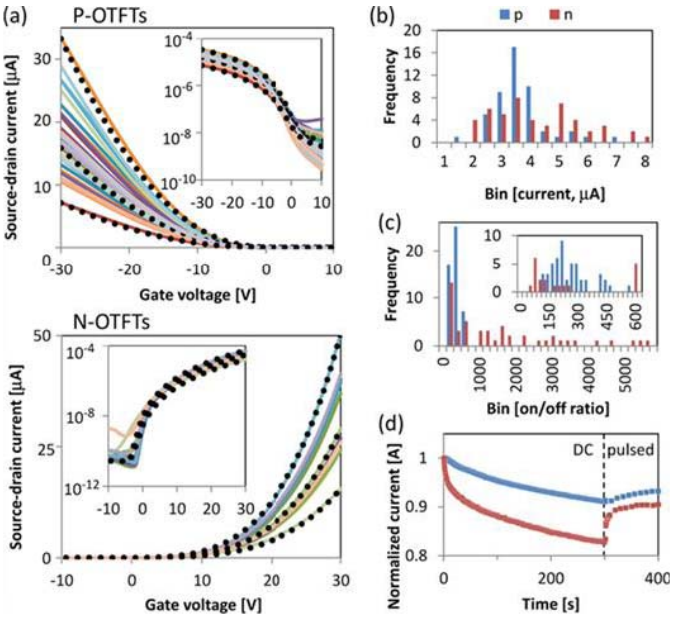

Fig. 1. (a) Transfer characteristics of printed p- and n-channel OTFTs, with channel width of 2.75 mm and length of 35 μm, in saturation regime Vds = $\pm$20 V and Vgs = $\pm$20 V. The dotted lines represent best-fit models for slow, typical, and fast OTFTs. Histograms of current distribution (b) and on/off ratio (c) were taken from measurements in linear regime Vds = $\pm$5 V and Vgs = $\pm$20 V for lower bound estimation. (d) Normalized current during operation with Vds = $\pm$20 V and Vgs = $\pm$20 V at constant gate bias or at pulsed gate bias of 1 kHz, 50% duty cycle. Reprinted with permission from [16].

systems typically use piezo-activated print-heads with many independently addressable ejectors and other types of print heads, such as aerosol jet and extrusion, are useful for fabricating hybrid systems. Fig. 2 shows a custom printing system developed at PARC [17]. The substrate is mounted on a translation stage and the print-heads are on an orthogonal stage; both stages have position accuracy of $\sim$1 μm. The printing system has a video image-capture system mounted near the print head, to locate previously printed alignment marks and software adjusts the drop ejection to provide approximately 5 μm registration. The printing accuracy ultimately depends on the performance of the print-head with regard to variations in drop directionality and velocity.

Ink-jet printing is an ideal printing technique for research and prototype development, but, in some cases, manufacturing may require higher throughput techniques such as gravure or other contact printing techniques. These techniques often give finer features, but typically have reduced layer-to-layer registration accuracy.

A challenge for ink-jet printed TFTs is the control of the liquid on the substrate surface. A hydrophobic surface tends to give small features, but the printed line may break up into droplets, while the feature size is large on a hydrophilic substrate, as the liquid spreads on the surface. In addition, an ink comprising a solute and a solvent that evaporates is subject to the coffee stain effect in which a large fraction of the solute is deposited at the edge of the drop rather than uniformly. Controlling these effects through ink-formulation and surface

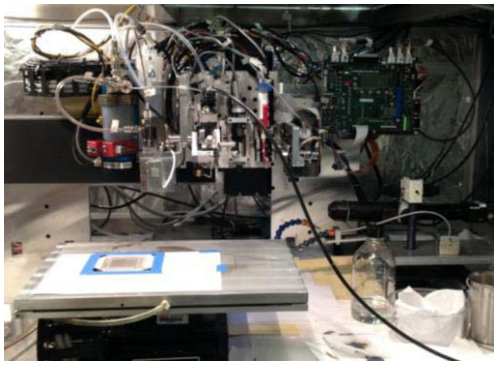

Fig. 2. Versatile apparatus for printed electronics with ink jet, aerosol jet and extrusion capability, UV curing, and an alignment camera.

chemistry is important to be able to make uniform printed TFTs with consistent circuit performance. Contact printing typically uses higher viscosity inks and the problem is reduced.

III. Electronic Circuit Design for Printed, Flexible Hybrid Electronics

Design of printed organic TFT circuits is affected to a great extent by the high degree of variability of printed organic TFTs. This includes both device-to-device variation associated with printing tolerances and inconsistent film formation, and temporal variation associated with bias stress as discussed above. In conventional silicon CMOS processes, variability tends to be low on neighboring devices and higher in more separated regions of a die or wafer, or among different wafers. In contrast, with print processing, and ink-jet fabrication in particular, variation is not significantly reduced through proximity.

A common design methodology for very-large-scale integration (VLSI) electronics uses process corners with separate models for "fast," "typical," and "slow" devices. Designs are simulated with combinations of p- and n-type models representing each corner to determine worst and best case performance. The effectiveness of this approach relies on the assumption that each die primarily consists of devices from a single process corner. An individual printed circuit, however, may contain any combination of devices from multiple corners. Therefore, while developing models for the extremes of performance is still helpful, careful consideration must be given to how variation in each device in a specific circuit will affect overall performance. Monte Carlo simulations are also a useful tool for gauging circuit functionality. In this technique, the likelihood of a circuit operating as designed can be assessed through repeated simulations with randomized parameter variations.

An additional effect of high device-to-device variability, in combination with the relatively low gain of printed TFTs, is that designing reliable analog circuits is difficult. The technique of "matching" nearby devices to form differential pairs, current mirrors, or bias circuits can be impractical while low gain limits the use of feedback to reduce sensitivity to variation. Consequently, with a few exceptions, most printed

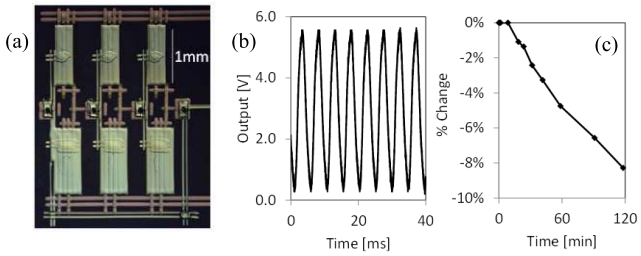

Fig. 3. (a) Micrograph of a three-stage ring oscillator circuit; (b) The voltage output with 6-V supply, and (c) the percent change in frequency over time.

circuits are digital logic circuits. There is a need for new design methodologies to enable reliable analog circuits.

Dedicated SPICE models are not generally available for organic TFTs. Typically, other TFT models, in particular the RPI amorphous silicon (a-Si) model, are used as they are functionally similar and have a sufficient degree of parametrization for development of reasonable fidelity in both the saturation and linear regimes. The models include empirical (i.e., non-physical) parameters and development of specific device models requires parameter extraction or curve fitting. While this approach enables the development of highly accurate models, in practice, for digital circuits, it is often not necessary to have perfect matching, especially in the subthreshold region. Physics-based models based on an assumed density of states have also been developed for organic TFTs, and reflect the unique characteristics of the materials [18].

A. Digital Circuits

Hole-conducting (p-type) organic semiconductors are more developed and stable than electron-conducting (n-type) materials. As a consequence, many leading research groups use exclusively p-type TFTs in their designs. This has led to several unipolar logic styles including with zero gate voltage loads, diode-connected loads, and "pseudo-CMOS" [19]. Complementary logic has an advantage for circuit design in that it allows for high inverter gain and rail-to-rail operation without requiring additional voltage rails. It also has a reduced sensitivity to bias stress [20]. In theory, it should also have lower power consumption than unipolar logic if high TFT on/off ratios are available.

The simplest digital circuit is the inverter. Several inverters wired together form a ring oscillator, which has become a standard circuit for benchmarking new devices. Ring oscillators allow evaluation of TFT speed, switching ratio, and bias-stress sensitivity. A printed ring oscillator and its performance are shown in Fig. 3. The unloaded oscillation frequency is initially 201 Hz, and degrades by 8% over 2 h because of reduction in current due to bias stress [21].

Another useful digital circuit is the address decoder. PARC worked with Thin Film Electronics to develop a circuit to address non-volatile printed memory arrays and reduce the overall pad count [16]. Fig. 4a shows a schematic of a 3-bit decoder unit comprising a 3-input NAND gate (M1-M6), two inverting buffers (M7/M8, M9/M10), and two transmission gates (M11/M12, M13/M14), for a total of fourteen OTFTs.

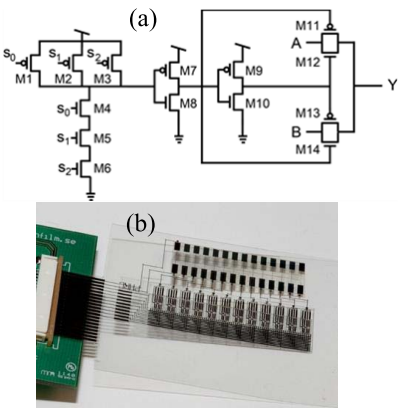

Fig. 4. (a) Schematic of one of eight decoder units; (b) photograph of a full 3-bit decoder (with four excess decoder units), connected to printed memory. Reprinted with permission from [16].

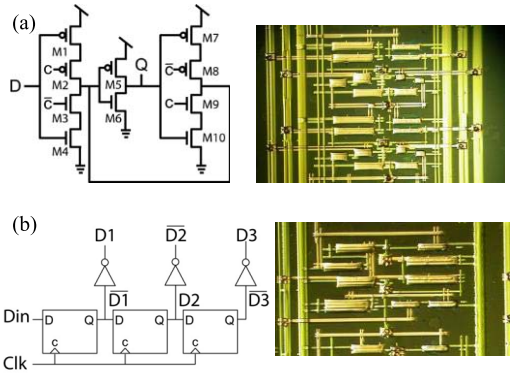

Fig. 5. Schematics and micrographs of (a) static and (b) dynamic flip-flop circuits used to form a shift register. Reprinted with permission from [22].

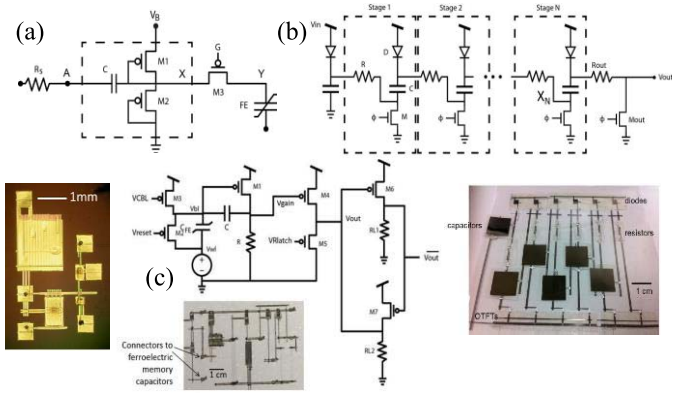

Fig. 6. Printed circuit examples: (a) pulse-generator; (b) voltage multiplier; (c) charge amplifier. Reprinted with permission from [23] and [24].

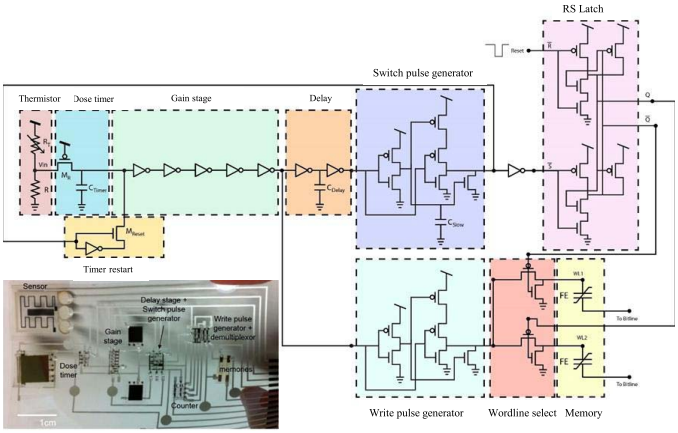

Fig. 7. Printed time-temperature dose tag showing the different sub-circuits and a photograph of the device. Reprinted with permission from [25].

This circuit passes either signal A or signal B to the output Y depending on the values of control signals s0, s1, and s2. The full decoder line, shown in Fig. 4b connected to a memory array, consists of eight of these units. The additional four units in the printed decoder are redundant and aid in yield mitigation.

Flip-flops represent another important digital circuit block with many uses ranging from temporary data storage to state-machine implementations. Fig. 5 shows examples of printed static and dynamic (i.e., clocked) flip-flop implementations used as the basis of shift register circuits [22]. The static design is fully latched and retains its state indefinitely, and is less impacted by clock feedthrough. However it uses a greater number of TFTs and requires complementary clock signals. The dynamic design, based on a true single-phase clock, has floating nodes and retains its state for approximately 25 ms. In simulation, the dynamic circuit consumes more power, except at relatively high clock frequencies.

B. Towards Analog Circuit Design

Circuit designers can leverage analog effects to reduce TFT count or achieve functional targets. For example, the pulse-generator circuit in Fig. 6(a) uses a clamped high-pass filter to generate a voltage pulse at nodes X and Y from a rising edge at node A. This circuit uses only three unipolar TFTs and a capacitor. A conventional monostable multivibrator would require six or seven TFTs in a complementary process to achieve a similar function [23]. Fig. 6(b) shows a voltage multiplier circuit consisting of printed TFTs, diodes, and capacitors. This circuit was designed to generate a high-voltage pulse from a lower-voltage supply, for example a 15 V pulse with a 9 V supply [24].

The circuit in Fig. 6(c) is a charge amplifier designed for reading a ferroelectric memory device C_{FE}. The charge on the memory cell is converted to a voltage with a single-TFT gain stage (M1 and R), and then latched. With conventional electronics, this function is typically performed by a high-gain sense amplifier or similar circuit. While such a circuit is currently not feasible in reasonable yield in an all-printed process, by designing towards the specific requirements of the application, the desired functionality is achieved with a much simpler circuit. Such an approach is fundamental to printed circuit design.

C. Complex Circuits: Smart Label

Functional circuit blocks are combined to enable complex functionality. The circuit in Fig. 7 is a time-temperature dose (TTD) tag that writes to memory the number of TTDs

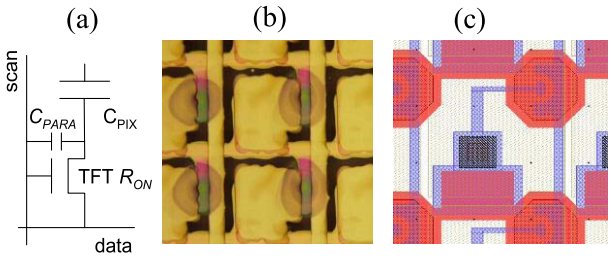

Fig. 8. (a) The pixel circuit of a TFT backplane. (b) Photograph of a portion of a printed TFT backplane. (c) Design of a pixel TFT with asymmetrical source and drain contacts so that the pixel parasitic capacitance is minimized.

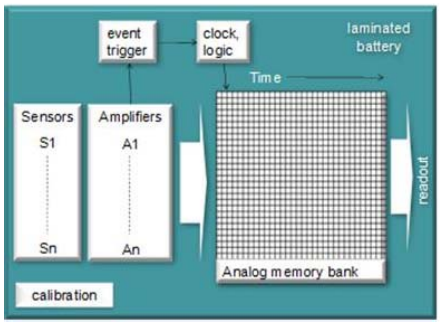

Fig. 9. Block diagram schematic of blast dosimeter wearable patch, comprising sensors, digital and analog electronics, analog memory and a power source.

to which the tag has been exposed, where a TTD is a temperature-weighted time interval, with reduced intervals for higher temperatures. TTD count is an important indicator of spoilage, for example of medicine or food. The circuit contains a number of sub-circuits including a resettable timer, a delay line, a gain stage, two pulse generators with different output characteristics, and an RS latch. The output is thermometer-coded on two memory bits. Extension to larger memories can be accomplished by replacing the latch with a shift register [25].

IV. Sensor Systems

Sensor arrays represent an important emerging application of printed organic electronics. They benefit from several attributes of print fabrication, including large area coverage and customizability. Sensor arrays can be of a single sensor modality, such as photosensors, pressure sensors, strain sensors, electrochemical and/or gas sensors, or a combination of multiple sensing types.

A. Optical sensor active matrix arrays

Various active matrix image sensor arrays have been fabricated with organic TFTs, organic photodiodes, printed devices and flexible substrates [26]. The pixel circuit is usually simple and comprises a photodiode and a TFT connected to the matrix of scan and data lines, which is essentially the same as the backplane of an LCD and is shown in Fig. 8. The matrix addressing places requirements on the TFT mobility, on/off ratio and parasitic capacitance [27]. The pixel addressing and hold times are

$$\tau_{AD} = R_{ON}C_{PIX}; \quad \tau_{HOLD} = R_{OFF}C_{PIX} \tag{1}$$

where R_{ON} and R_{OFF} are the on and off resistance of the TFT and C_{PIX} is the pixel capacitance. The TFT parasitic capacitance, C_{PARA}, modifies the pixel voltage though the capacitive charge transferred when the gate voltage is switched. This feedthrough voltage is

$$\Delta V = V_G C_{PARA}/C_{PIX}. \tag{2}$$

The typical requirement is to address the pixel in a few microseconds, yet hold the charge without loss for ~1 second. A TFT is required with a high on/off ratio of about 10^7, but a mobility of ~1 cm^2/Vs is usually sufficient to address an array at video rates. A small feedthrough voltage requires low parasitic capacitance. Organic TFTs satisfy the mobility and on/off ratio, but high parasitic capacitance can be an issue for printed devices, because of the large size of the printed features. A large feedthrough voltage can sufficiently alter the bias on the photodiode and TFT to distort the signal. An example of a printed backplane pixel is shown in Fig. 8. In a typical active matrix array, the low parasitic capacitance is only needed on the pixel side of the TFT because the feedthrough voltage affects the LCD or photodiode response but has minimal effect on the address lines. Hence, an asymmetric source-drain contact design can be used to optimize the circuit performance as illustrated in Fig. 8. This type of asymmetrical design is typical for conventional LCDs.

B. Printed Sensor System With Analog Memory

Another example of a complex POE system developed at PARC is the wearable blast dosimeter, a project to design and create a flexible electronic patch on a soldier's helmet to record the exposure to explosive blasts and monitor for possible brain trauma [28]. The electronic circuit was designed to monitor various pressure, acceleration and light sensors, record their transient response during an event, and store the data in a local memory before periodic read out. The circuit schematic is shown in Fig. 9 and was designed with both analog and digital electronics and memory, as well as the various sensors. The circuit required buffer amplifiers for the sensor, data memory, clock, logic and trigger circuit elements. Circuit challenges included designing printed sensors with an electrical response that is compatible with the printed TFTs forming the buffer, developing a printable memory circuit, and keeping the device count low for small area and reasonable yield.

The high operating voltage and high impedance of printed organic TFTs led to the choice of piezoelectric pressure sensors and accelerometers. The organic piezoelectric and ferroelectric material poly(vinylidene fluoride-trifluoroethylene) (PVDF-TrFE) was chosen because it a has a high voltage response and high impedance, simplifying the design of the buffer amplifiers. The sensors are formed as a PVDF-TrFE film laminated over a cavity with printed the electrical contacts [29]. The pressure sensor is a sealed cavity and the accelerometer is the same structure with a printed proof mass. The PVDF co-polymer sensors have a

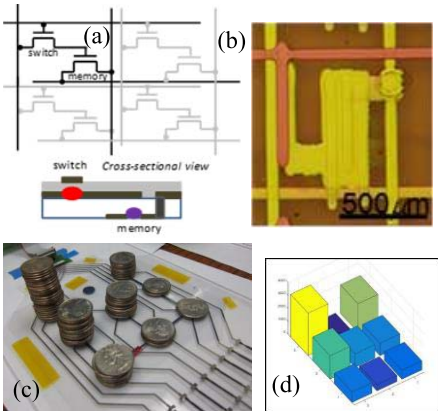

Fig. 10. (a) Pixel design and device cross-section of a memory pixel comprising a PVDF-TrFE ferroelectric memory TFT and a conventional switching TFT. (b) Optical micrograph of the memory pixel. (c) An eight pixel printed resistive pressure sensor array with test masses. (d) Readout from the pressure sensor array.

comparable response to conventional pressure sensors and accelerometers, although with reduced signal-to-noise. Making all the sensors with PVDF-TrFE has the advantage that the electronic response is similar in each case and can therefore be amplified and stored by the same analog circuitry.

The memory array circuit was also a design adapted to the specific capability of printed electronics. Digital memory has significant disadvantages for printed devices because each channel needs an analog-to-digital A/D converter which is a complex circuit, and bit-wise storage also involves a large number of storage elements. An analog memory was chosen because it does not require an A/D and has fewer memory cells. The active matrix circuit has a 2-TFT memory element shown in Fig. 10, with an address TFT and a ferroelectric memory TFT which has PVDF-TrFE as the gate dielectric [30]. The ferroelectric polarization induced during the write cycle encodes the sensor voltage in the gate bias of the device and PVDF-TrFE characteristics match the operational voltage of the memory element to that of the sensors. The conventionally-designed address TFT controls the voltage path to each pixel switch and allows a specific memory cell to be accessed during read and write operations. The ferroelectric memory has a signal-to-noise ratio exceeding 25 on the first day after writing, reducing to about 10 after 14 days due to the charge-trapping effect in the ferroelectric TFT [31].

Printed pressured sensors can also be capacitive or resistive rather than ferroelectric. Fig. 10(c) and (d) show a pressure sensor array printed at PARC, using a carbon-based resistive sensing material. Pressure sensor arrays have numerous applications in healthcare, retail, industrial processes, user interfaces and artificial skin [32].

C. Smart Sensor Tags With Hybrid RF Communication

Wireless communication of sensor signals is essential for realizing many useful distributed sensing applications. While some examples have previously been demonstrated [33], radio frequency (RF) communication using printed circuits is not currently practical due to the material properties and print resolutions associated with these devices which typically

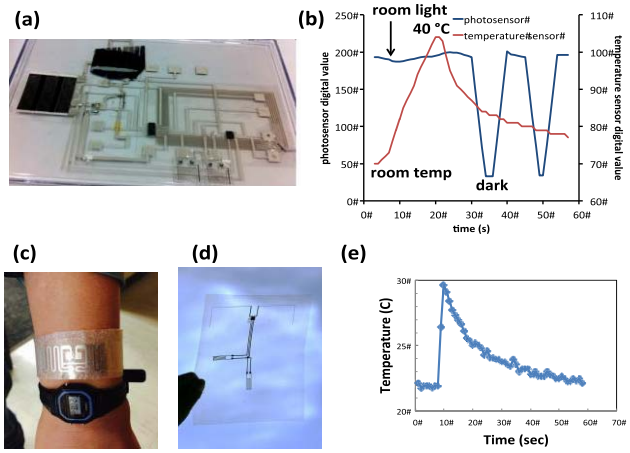

Fig. 11. (a) Image of a complete printed wireless light and temperature sensor system using fabricated on a flexible substrate having a printed light sensor, temperature sensor, multiplexing transistors, antenna and other passives (resistors, capacitors) and pre-fabricated chips for RF communication and sensor signal processing. (b) Output of the sensor system show in (a). (c) Passively powered flexible wireless temperature sensor system based on an AMS SL900A chip (system shown using a bare-die on flex). (d) Strain sensor system on flexible incorporating printed strain sensors and antenna with a packaged SL900A chip. (e) RF powered output of a printed temperature sensor tag based on an SL900A chip.

result in low operational frequencies. A hybrid approach that combines printed devices with pre-fabricated microelectronic components overcomes this issue. Such an approach provides a method for achieving complex functionality using the large library of existing commercially available components while maintaining many of the benefits of printed devices—including facile customization, large area coverage, and high sensitivity detection.

Mechanical and electrical integration are the primary issues that must be considered when following this hybrid approach. The elastic modulus mismatch between soft, organic, mechanically flexible substrates (e.g., polyesters) and rigid pre-fabricated chips must be overcome to provide systems which are reliably mechanically flexible. Various methods have been demonstrated to achieve this goal including flexible interconnects [34], as well as making the microelectronic components themselves flexible though thinning [35]. Electrical integration can also be a significant issue as printed devices typically have limited resolution (minimum feature size and spacing on the order of 10s of microns) and often require thick films to prevent leakage through dielectric layers that overcoat rough printed metals. These properties can lead to large impedance and to operating voltages for some printed devices which are higher than the supply voltages typically required for microelectronic components. In order to avoid undesirable additional complexity, developing printed components capable of operation at 3–5 V is important when mixing silicon dies with printed components. For example, bilayer dielectrics composed of low and high-k fluoropolymers which provide a low energy semiconductor-dielectric interface with a high overall capacitance, printed organic TFTs have been fabricated that operate at 3.6 V, and have been shown to be suitable for multiplexing printed sensor signals to the analog input of a PIC microcontroller (Fig. 11) [17], [36].

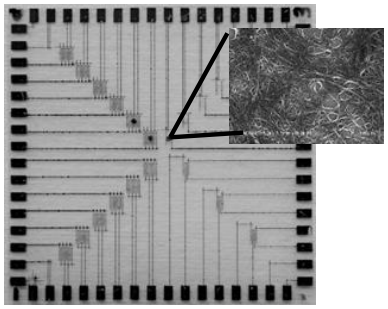

Fig. 12. Printed carbon nanotube gas sensor test array.

A design approach that minimizes the number of discrete components (ideally to a single device) while maximizing the number of printed devices is desirable as it simplifies fabrication, maintains the benefits of print-based manufacturing and facilities mechanical flexibility. As such, careful component selection and circuit design is critical. For example, antennas for RF communication need to be impedance-matched to the wireless IC being used. This is often achieved using a network of passive devices, which can be difficult when using passives printed from solution-based inks since the range and precision of resistances, inductances and capacitances that they are able to easily provide is limited in comparison with what is available from discrete components.

To eliminate these complex networks while maintaining performance, antennas can be designed specifically to impedance-match the wireless chip used without the need for any passive components. An example is shown in Fig. 11. Here a number of antenna designs were simulated, fabricated and tested to match the 31-320j Ω, input impedance of an AMS SL900A data logger chip, allowing the device to be fabricated without the need for any ancillary passive components. This particular device demonstrates an example of a simple system layout. This chip can be powered wirelessly through energy harvested from the reader, meaning that no on-board power source is required for operation. Printed strain and touch sensors were designed to be read directly by the analog inputs of the chip, and the antenna was impedance matched to the chip. This provides a simple stand-alone hybrid printed flexible platform system for wirelessly reading sensor states.

D. Gas Sensing

Gas and chemical sensing is another set of applications that can benefit from POE. Gas sensing is important for leak detection, indoor and outdoor air quality monitoring, industrial and residential safety, and other uses. Fig. 12 shows a test array used for developing a printed natural gas leak detector based on printed carbon-nanotube (CNT) sensors. Each chemiresistive sensor element is formed of sensor material dispenser-printed on interdigitated printed electrodes. The sensor elements comprise CNTs modified with dopants, coatings, or nanoparticles such that they responds differently to different gases. While each sensor material can be extremely sensitive (down to 250-ppb methane, for example), selectivity is achieved through the combined response from multiple materials. Materials have been identified with sensitivity to many different gases, including methane, general volatile organic compounds, ammonia, hydrogen sulfide, carbon monoxide, chlorine, and hydrogen, among others. Printing enables simple customization to different target and interfering gases, redundancy to reduce noise and improve yield, and low-cost replacement after prolonged exposure to harsh environmental conditions. The array can be augmented with printed temperature, humidity or other sensors for calibration or additional functionality.

V. Electrochemical Sensing

Organic electronic devices and flexible printed electronics are increasingly being developed for health monitoring based on electrochemical sensing. Sensing elements for such biological and environmental detection can broadly be classified into two main areas: analyte detection, and measurements of local potentials for electrophysiology.

A broad range of sensors perform signal transduction by utilizing electrochemically active materials and selective binding moieties. Analyte sensing, i.e., the detection of specific ions or biomolecules relies on specific binding interactions, and can lead to detected changes in surface or bulk charge. Capture or sensing of ions benefits from decades of research surrounding ion selective membranes used as electrode coatings or membranes for ion selective FETs (ISFETs) [37]. These membranes can be useful for biological and environmental sensing applications in aqueous environments, the selectivity of which is dictated by the chemistry of the active site–the ionophore [38]. Biomolecule detection depends on selective capture through a binding interaction (facilitated by either enzymatic or DNA detection) leading to direct charging of an interface or indirect charge transfer through an intermediary. Alternatively, biomolecule detection can be achieved by sensing of the electrochemical signature of the molecule through modified cyclic voltammetry [39]. Electrophysiology measurements, on the other hand, do not detect specific binding events or molecular fingerprints, but instead the local changes in field potentials due to the activity of electroactive cells (i.e., muscle, nerve, or neuronal tissue), or due to changes in ionic fluxes.

A. Electrochemical Transistors for Analyte Sensing

Transistors can be pivotal sensing elements when the desired signal is small. The transistor's inherent gain can allow the interfacial sensing element to act effectively as an amplifying transducer. In this case, the channel of the transistor is brought into direct contact with the sensing environment, such that the local change in potential, small changes in ion currents, or binding of charged molecules directly modifies the conductance of the transistor channel. This is approach is well known in ISFETs, and other (bio-functionalized) organic and inorganic FETs utilized in numerous applications [40], [41].

Conducting polymer materials have recently been targeted as active channel materials in transistors owing to their mixed conduction properties. Unlike field effect transistors, where channel conductance is modulated electrostatically, devices based on conducting polymers depend on the bulk electrochemical doping of the conjugated polymer. These Organic Electrochemical Transistors (OECTs) [42] have found applications in biosensing due to their soft mechanical properties,

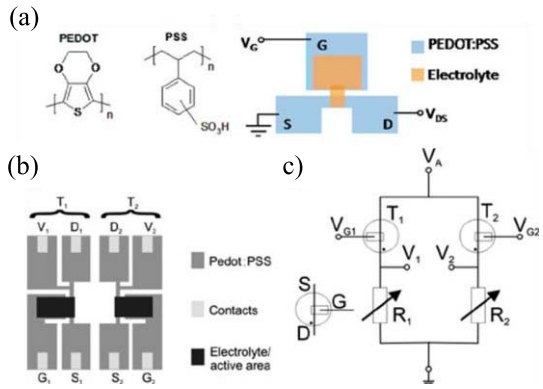

Fig. 13. (a) Materials and layout of a co-planar organic electrochemical transistor based on the conducting polymer dispersion PEDOT:PSS. Wiring is as denoted. The source (S), drain (D), and gate (G) contacts are all made of PEDOT:PSS, the electrolyte between the source and drain define the active channel of the OECT. (b) Layout and c. circuit diagram for a Wheatstone bridge sensing circuit utilizing two OECTs (a sensing and reference transistor) used in ion sensing experiments. Reprinted with permission from [47].

fabrication on flexible and conformal substrates, and free exchange of ions with the active material. While OECTs share many aspects in common with their electrolyte gated FET counterparts, their bulk doping leads to high effective capacitance yielding high transconductance at low operating voltages [43]. OECTs are sensitive electrophysiology transducers [44], and have utilized similar functionalization approaches described above to enhance transduction of signals in ion sensing and biomolecule sensing [45]. Nevertheless, the same ion penetration that has proven advantageous for OECTs compared to electrolyte gated FETs, can lead to problems in reversibility or degradation, and slower device response times, the importance of which depends on the time scale of the targeted biological event.

Fig. 13 shows the OECT device and a circuit example. The specific device design requirements depend on the application space targeted. An electrophysiology sensor, for example requires that the gate electrode serves as the ground/reference electrode. If the measurement is performed in contact with biological media, where a non-zero voltage drop can have deleterious effects, the OECT must be designed through materials or device engineering to have its peak sensitivity (operating bias) at a gate offset near 0 V [46].

With electrochemical transistors, especially those based on PEDOT:PSS, a major concern for circuit design is that the devices show high ($>$1 mA) currents in their unbiased state. The depletion-mode operation of these transistors means that they are "ON" at a gate bias of 0 V, and that during recording, the baseline current can be high. This complicates sensing low level electrophysiology when there might be a 10 μA signal on top of a mA background, and requires signal conditioning circuitry to interface with commercial amplifiers such as the approach used by Yao et al. [48]. Since the OECT effectively measures a change in the resistance of PEDOT:PSS due to the local ionic fluxes in the sensing environment, some researchers have utilized bridge circuits for sensitive analyte detection. One notable example of this approach was utilized by Svensson, et al. for ion sensing (see Fig. 13) [47].

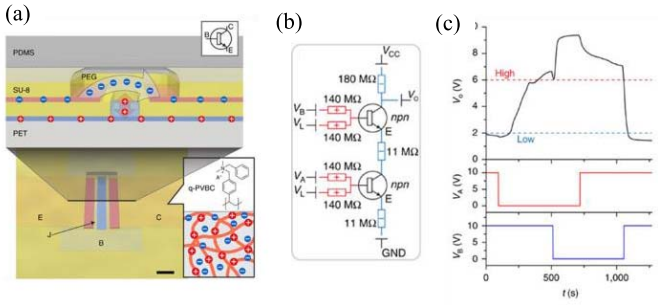

Fig. 14. (a) Ion bipolar junction transistor, utilizing ion diffusion and electrophoretic transport through polycations/anions. The emitter (E), collector (C), junction (J), and base (B) are indicated. (b) Circuit diagram for an npn-IBJT based NAND gate. (c) The resulting NAND gate characteristics. Reprinted with permission from [56].

When a sensing element must be in direct contact with a fluid, notably for most applications where electrochemical or direct binding events are required for signal transduction, the fabrication is complicated. The supporting circuitry, whether printed or thin film electronics or hybrid silicon CMOS chips, must be encapsulated in a reliable way, while allowing for the sensing element to be exposed. While a number of routes to encapsulate supporting electronics have been developed, including encapsulation in polyimide, parylene C, and elastomers [43], [49], [50], the challenge remains that the sensing surface must usually be functionalized as a final step in the fabrication. The pathways for device failure are also enhanced when encapsulation is not continuous and hermetic. Exposed sensing sites may present facile routes for fouling, delamination, and ultimately failure [51], [52].

B. Iontronics

A rising area of sensing and biochemical stimulation aims to replace or minimize the role of electronics with materials and devices based on ionic fluxes. So-called iontronics, utilizing proton hopping and ion-based logic, has received significant attention [53], [54]. In addition to the recent demonstration of protonic transistors utilizing synthetic and natural polymers such as proteins, all ion-based circuits have been demonstrated [54]–[56]. Such iontronic circuits are based on integrated chemical logic gates composed of ion bipolar junction transistors [56]. The inverters and NAND gates are based entirely on the motion of ions in an electrolyte and electrophoretic transport through specially selected polyanionic and polycationic materials as illustrated in Fig. 14 [57]. The authors claim that such work will lead to active solid-state chemical delivery circuits for example, in smart petri-dish applications.

C. Electroded Sensors

Electrode based electrophysiology recordings are well established and are another opportunity for organic electronic circuits. When sensing a potential, a partner electrode is required, which can commonly be a single global ground. For electrochemical-based measurements a typical three electrode configuration is desired—this can be achieved with a fully integrated potentiostat-like approach—with a working, counter

and reference electrode. The working electrode supports a biological reaction such as that of glucose and glucose oxidase, and defines the specificity of the sensor. A true three-electrode measurement requires a high-gain feedback element, which is challenging to achieve with all-printed devices. Alternatively, the bias dependent changes in current can be recorded to deduce the local electrochemical environment at the working electrode, similar to cyclic voltammetry (CV). Fast scan CV can, for example, be used for local detection of neurotransmitters such as serotonin or dopamine [39]. Frequency dependent measurements can be utilized to measure local impedance, for example of skin or cultured cell layers [58], [59]. Such measurements require either a broad range of probed frequencies, or carefully selected input frequencies for probing. The supporting circuitry required for these applications depends on whether the analysis is performed on-board, or whether the data is meant for processing off line. Nevertheless, the measured currents ultimately depend on the impedance at the electrode-electrolyte interface. This impedance is dictated by the effective interfacial surface area of the electrode for inorganic materials (lowered by nanostructuring, for example in Pt, TiN, IrO), or by the bulk capacitance for soft electrode coatings (i.e., polymeric semiconductors/conductors or CNT forest electrode coatings) [60], [61].

VI. Summary

Flexible electronics based on organic TFTs has achieved working prototypes with suitable performance for several potential applications. Both circuit and sensing elements demonstrate good compatibility with fabrication methods, with reasonable stability when encapsulated and good operation under flexing. Circuits and systems made with these components are gaining attention. Hybrid integration with silicon ICs is an important technology component for many applications, particularly those requiring RF communication. Integrating multiple imaging and sensing modalities remains a technical challenge, as does the development of suitable power sources. The transition from demonstrator circuits to manufactured products is a further challenge.

Acknowledgment

The authors would like to acknowledge the contributions of many current and former members of the printed electronics effort at PARC and their many collaborators in other institutions.

References

[1] T. Sekitani *et al.*, "Stretchable active-matrix organic light-emitting diode display using printable elastic conductors," *Nature Mater.*, vol. 8, pp. 494–499, May 2009.

[2] M. Jung *et al.*, "All-printed and roll-to-roll-printable 13.56-MHz-operated 1-bit RF tag on plastic foils," *IEEE Trans. Electron Devices*, vol. 57, no. 3, pp. 571–580, Mar. 2010.

[3] J. W. Boley, E. L. White, and R. K. Kramer, "Mechanically sintered gallium-indium nanoparticles," *Adv. Mater.*, vol. 27, no. 14, pp. 2355–2360, Feb. 2015.

[4] K.-J. Cho, J. S. Koh, S. Kim, W. S. Chu, Y. Hong, and S. H. Ahn, "Review of manufacturing processes for soft biomimetic robots," *Int. J. Precis. Eng. Manuf.*, vol. 10, pp. 171–181, Jul. 2009.

[5] B. C.-K. Tee *et al.*, "A skin-inspired organic digital mechanoreceptor," *Science*, vol. 350, no. 6258, pp. 313–316, Oct. 2015.

[6] J. E. Anthony, A. Facchetti, M. Heeney, S. R. Marder, and X. Zhan, "N-type organic semiconductors in organic electronics," *Adv. Mater.*, vol. 22, no. 34, pp. 3876–3892, Sep. 2010.

[7] J. Li *et al.*, "A stable solution-processed polymer semiconductor with record high mobility for printed transistors," *Sci. Rep.*, vol. 2, Oct. 2012, Art. no. 754.

[8] R. A. Street *et al.*, "Sol-gel solution-deposited InGaZnO thin film transistors," *ACS Appl. Mater. Interfaces*, vol. 6, no. 6, pp. 4428–4437, Mar. 2014.

[9] Q. Cao *et al.*, "Medium-scale carbon nanotube thin-film integrated circuits on flexible plastic substrates," *Nature Int. Weekly J. Sci.*, vol. 454, pp. 495–500, May 2008.

[10] K. Myny *et al.*, "Unipolar organic transistor circuits made robust by dual-gate technology," *IEEE J. Solid-State Circuits*, vol. 46, p. 1224, May 2011.

[11] S. H. Kim *et al.*,, "Electrolyte-gated transistors for organic and printed electronics," *Adv. Mater.*, vol. 25, no. 13, pp. 1822–1846, Apr. 2013.

[12] C. Vanoni, S. Tsujino and T. A. Jung, "Reduction of the contact resistance by doping in pentacene few monolayers thin film transistors and self-assembled nanocrystals," *Appl. Phys. Lett.*, vol. 90, p. 193119, May 2007.

[13] R. A. Street, M. C. Chabinyc, F. Endicott, and B. Ong, "Extended time bias stress effects in polymer transistors," *J. Appl. Phys.*, vol. 100, p. 114518, Dec. 2006.

[14] R. A. Street, M. C. Chabinyc, and F. Endicott, "Chemical impurity effects on transport in polymer transistors," *Phys. Rev. B*, vol. 76, p. 045208, Jul. 2007.

[15] Y. Mei *et al.*, "High mobility field-effect transistors with versatile processing from a small-molecule organic semiconductor," *Adv. Mater.*, vol. 25, pp. 4352–4357, Apr. 2013.

[16] T. N. Ng *et al.*, "Scalable printed electronics: An organic decoder addressing ferroelectric non-volatile memory," *Sci. Rep.*, vol. 2, Aug. 2012, Art. no. 585.

[17] R. A. Street *et al.*, "From printed transistors to printed smart systems," *Proc. IEEE*, vol. 103, no. 4, pp. 607–618, Apr. 2015.

[18] F. Torricellia *et al.*, "Unified drain-current model of complementary p- and n-type OTFTs," *Organic Electron.*, vol. 22, pp. 5–11, Jul. 2015.

[19] Y. Takada, Y. Yoshimura, Y. Kobayashi, D. Kumaki, K. Fukuda, and S. Tokito, "Integrated circuits using fully solution-processed organic TFT devices with printed silver electrodes," *Organic Electron.*, vol. 14, pp.3362–3370 Dec. 2013.

[20] H. Sirringhaus, "Device physics of solution-processed organic field-effect transistors," *Adv. Mater.*, vol. 17, no. 20, pp. 2411–2425, Oct. 2005.

[21] N. T. Nga *et al.*, "Comparison of conductor and dielectric inks in printed organic complementary transistors," *Proc. SPIE*, vol. 9158, p. 91850, Oct. 2014.

[22] D. E. Schwartz and T. N. Ng, "Comparison of static and dynamic printed organic shift registers," *IEEE Electron Device Lett.*, vol. 34, no. 2, pp. 271–273, Feb. 2013.

[23] D. E. Schwartz *et al.*, "Comparison of organic pulse-generator circuits for ferroelectric memories fabricated by all-additive printing," *ECS Trans.*, vol. 54, pp. 165–170, 2013.

[24] T. N. Ng *et al.*, "Pulsed voltage multiplier based on printed organic devices," *Flexible Printed Electron.*, vol. 1, p. 015002, Dec. 2015.

[25] T. N. Ng *et al.*, "Printed dose-recording tag based on organic complementary circuits and ferroelectric nonvolatile memories," *Sci. Rep.*, vol. 5, Aug. 2015, Art. no. 13457.

[26] T. N. Ng, W. S. Wong, M. L. Chabinyc, S. Sambandan, and R. A. Street, "Flexible image sensor array with bulk heterojunction organic photodiode," *Appl. Phys. Lett.*, vol. 92, p. 213303, 2008.

[27] R. A. Street, "Thin-film transistors," *Adv. Mater.*, vol. 21, pp. 2007–2022, May 2009.

[28] A. Arias *et al.*, "Flexible printed sensor tape based on solution processed materials," in *Proc. 23rd Annu. Meeting IEEE Photon. Soc.*, Nov. 2010, doi: 10.1109./PHOTONICS.2010.5698733.

[29] J. H. Daniel, T. N. Ng, J. Coleman, J. Liu, and R. Jackson, "Pressure sensors for printed blast dosimeters," in *Proc. IEEE Sensors Conf.*, Nov. 2010, pp. 2259–2263.

[30] T. N. Ng, B. Russo, B. Krusor, R. Kist, and A. C. Arias, "Organic inkjet-patterned memory array based on ferroelectric field-effect transistors," *Organic Electron.*, vol. 12, pp.2012–2018, Dec. 2011.

[31] T. N. Ng, B. Russo, and A. C. Arias, "Degradation mechanisms of organic ferroelectric field-effect transistors," *J. Appl. Phys.*, vol. 106, p. 094504, Nov. 2009.

[32] T. Someya *et al.*, "A large-area, flexible pressure sensor matrix with organic field-effect transistors for artificial skin applications," *Proc. Nat. Acad. Sci. USA*, vol. 101, p. 9966, Mar. 2004.
[33] M. Jung *et al.*, "All-printed and roll-to-roll-printable 13.56-MHz-operated 1-bit RF tag on plastic foils," *IEEE Trans. Electron Devices*, vol. 57, pp. 571–580, Mar. 2010.
[34] S. Yu *et al.*, "Soft Microfluidic Assemblies of Sensors, Circuits, and Radios for the Skin Science etc.," vol. 344, pp. 70–74, 2014.
[35] D. Shahrjerdi, S. W. Bedell, "Extremely flexible nanoscale ultrathin body silicon integrated circuits on plastic," *Nano Lett.*, vol. 13, pp. 315–320, Jan. 2013.
[36] G. L. Whiting, "Combination of printed sensors and transistors with silicon components for digitally fabricated hybrid multi-modal sensing systems," *to be published*.
[37] R.P. Buck, "Ion selective electrodes," *Anal. Chem.*, vol. 50, pp. 17–29, 1978.
[38] P. Buhlmann, E. Pretsch, and E. Bakker, "Carrier-based ion-selective electrodes and bulk optodes. 2. ionophores for potentiometric and optical sensors," *Chem. Rev.*, vol. 98, pp. 1593–1687, Jun. 1998.
[39] D. L. Robinson, B. J. Venton, M. L. Heien, and R. M. Wightman, "Detecting subsecond dopamine release with fast-scan cyclic voltammetry in vivo," *Clin. Chem.*, vol. 49, pp. 1763–1773, Oct. 2003.
[40] L. Torsi, "Organic field-effect transistor sensors: A tutorial review," *Chem. Soc. Rev.*, vol. 42, pp. 8612–8628, Sep. 2013.
[41] P. Fromherz, A. Offenhauser, T. Vetter, and J. Weis, "A neuron-silicon junction: A retzius cell of the leech on an insulated gate field effect transistor," *Science*, vol. 252, pp. 1290–1293, May.1991.
[42] D. Nilsson, M. Chen, T. Kugler, and T. Remonen, "Bi-stable and dynamic current modulation in electrochemical organic transistors," *Adv. Mater.*, vol. 14, pp. 51–54, Jan. 2002.
[43] D. Khodagholy *et al.*, "High transconductance organic electrochemical transistors," *Nat. Commun.*, vol. 4, Jul. 2013, Art. no. 2133.
[44] J. Rivnay *et al.*, "High-performance transistors for bioelectronics through tuning of channel thickness," *Sci. Adv.*, vol. 1, p. e1400251, May 2015.
[45] X. Strakosas, M. Bongo, and R. M. Owens, "The organic electrochemical transistor for biological applications," *J. Appl. Polym. Sci.*, vol. 132, p. 41735, Apr. 2015.
[46] J. Rivnay *et al.*, "Organic electrochemical transistors with maximum transconductance at zero gate bias," *Adv. Mater.*, vol. 25, pp. 7010–7014, Dec. 2013.
[47] P. O. Svensson, D. Nilsson, R. Forchheimer, and M. Berggren, "A sensor circuit using reference-based conductance switching in organic electrochemical transistors," *Appl. Phys. Lett.*, vol. 93, p. 203301, Nov. 2008.
[48] D. Khodagholy, "Highly conformable conducting polymer electrodes for in vivo recordings," *Adv. Mater.*, vol. 23, pp. H268–H272, Sep. 2011.
[49] D.-H. Kim *et al.*, "Epidermal electronics," *Sci.*, vol. 333, no. 6044, pp. 838–843, 2011.
[50] S. Xu *et al.*, "Soft microfluidic assemblies of sensors, circuits, and radios for the skin," *Science*, vol. 344, pp. 70–74, Apr. 2014.
[51] L. A. Geddes and R. Roeder, "criteria for the selection of materials for implanted electrodes," *Ann. Biomed. Eng.*, vol. 31, pp. 879–890, Jul. 2003.
[52] J. C. Sanchez, *Neuroprosthetics: Principles and Applications*. Boca Raton, FL, USA: CRC Press, 2015.
[53] J. Leger, M. Berggren, and S. Carter, *Iontronics: Ionic Carriers in Organic Electronic Materials and Devices*. Boca Raton, FL, USA: CRC Press, 2010.
[54] Z. Hemmatian *et al.*, "Taking electrons out of bioelectronics: Bioprotonic memories, transistors, and enzyme logic," *J. Mater. Chem. C*, vol. 25, pp. 6407–6412, Apr. 2015.
[55] D. D. Ordinario *et al.*, "Bulk protonic conductivity in a cephalopod structural protein," *Nature Chem.*, vol. 6, pp. 596–602, Jun. 2014.
[56] K. Tybrandta, K. C. Larssonb, A. R. Dahlforsb, and M. Berggrena, "Ion bipolar junction transistors," *Proc. Nat. Acad. Sci. USA*, vol. 107, pp. 9929–9932, Apr. 2010.
[57] K. Tybrandt, "Logic gates based on ion transistors," *Nature Commun.*, vol. 3, May 2012, Art. no. 871.
[58] S. L. Swisher *et al.*, "Impedance sensing device enables early detection of pressure ulcers in vivo," *Nature Commun.*, vol. 6, Mar. 2015, Art. no. 6575.
[59] I. Giaever and C. R. Keese, "A morphological biosensor for mammalian cells," *Nature*, vol. 366, p. 591, Dec. 1993.
[60] P. Fattahi, G. Yang, G. Kim, and M. R. Abidian, "A review of organic and inorganic biomaterials for neural interfaces," *Adv. Mater.*, vol. 26, pp. 1846–1885, Mar. 2014.
[61] E. Castagnola *et al.*, "Smaller, softer, lower-impedance electrodes for human neuroprosthesis: A pragmatic approach," *Front. Neuroeng.*, vol. 7, p. 102, Apr. 2014.

David E. Schwartz received the B.S. degree in mathematics from Brown University, Providence, RI, USA, and the Ph.D. degree in electrical engineering from Columbia University, New York, NY, USA.

He has a background in mixed-signal CMOS circuit design with research interests in energy and printed electronics. In the printed electronics area at PARC, he has applied his expertise in device modeling and circuit design and testing to printed organic electronics technology.

Jonathan Rivnay received the B.S. degree from Cornell University, Ithaca, NY, USA, and the M.S. and Ph.D. degrees from Stanford University, Stanford, CA, USA.

Prior to joining PARC, he was a Marie Curie postdoctoral fellow in the Department of Bioelectronics in the Centre Microelectronique de Provence in France. At PARC he is developing sensor materials and devices for health monitoring and bioelectronics applications.

Gregory L. Whiting received the B.S. degree from the University of California, Berkeley, CA, USA, the Ph.D. degree from the University of Cambridge, Cambridge, U.K.

His research interest is in novel materials, fabrication/patterning methods, and applications for electronic systems. His work focuses on electronic devices that can be print processed from solution for applications such as mechanically flexible active-matrix backplanes and sensor systems. Other research includes electric-field driven digital fluidic assembly of microelectronic components, 3D printed electronics, and transient electronic systems.

Ping Mei received the B.S. degree in physics from Peking University, Beijing, China, and the Ph.D. degree in physics from Rutgers University, New Brunswick, NJ, USA.

She has worked at PARC and HP Labs and is currently working on developing printed electronics for digital processing and device integration toward low-cost manufacturing fabrication and novel device applications.

Yong Zhang received the B.S. and M.S. degrees in mechatronics engineering from Harbin Institute of Technology, Harbin, China, and the Ph.D. degree in electrical and computer engineering from the University of Toronto, Toronto, ON, Canada.

Prior to joining PARC, Yong was a Research Engineer at Georgia Institute of Technology. His research is focused on the development of additive manufacturing technologies, design and fabrication of microdevices, and microrobotic manipulation.

Brent Krusor received the B.S. degree in chemistry from the Massachusetts Institute of Technology, Cambridge, MA, USA, and the M.S. degree in physical chemistry from the University of California, Berkeley, CA, USA.

His recent research concerns inkjet printing of organic electronic materials to create flexible, large-area transistor and sensor arrays.

Sivkheng Kor is a Research Assistant at PARC. She is focused on developing printing processes for printed organic electronics devices and also develops conventional photo-lithography processes for research projects.

George Daniel received the B.S. degree in engineering from Syracuse University, Syracuse, NY, USA.

Prior to joining PARC, he was the Principal Engineer for Accurate Electronics, where he integrated wireless capability into GE Energy's smart meters. His areas of expertise include metamaterials in the microwave band, wireless communication, transceiver architecture, sensor networks, power conversion, antenna design, and radar systems.

Steve E. Ready received the degree in physics from the University of California, Santa Cruz, CA, USA.

He joined PARC shortly after receiving the degree. He has designed and developed inkjet printers for printed organic electronics, and contributed to the development of large-area amorphous and polycrystalline silicon arrays for optical and X-ray imaging, displays, and organic semiconductor materials and devices.

Janos Veres received the Ph.D. degree in solid state electronics from Imperial College, London, U.K.

He has held R&D and manufacturing management positions in material, printing and electronics companies including PolyPhotonix, Kodak, Merck, Avecia, and Gestetner, where he developed printed circuits, specialty functional materials, OLEDs, displays, medical devices as well as printing/coating technologies. His main interest is exploring 2D and 3D printing as a manufacturing technique for electronic devices.

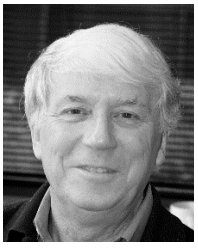

Robert A. Street received the Ph.D. degree in physics from Cambridge University, Cambridge, U.K.

He worked at Sheffield University and the Max Planck Institute in Stuttgart before joining the Palo Alto Research Center where he is now a Senior Research Fellow. His research has focused on large area electronics, including amorphous silicon, flat panel X-ray image sensors, printed organic semiconductors, flexible electronics and organic solar cells.